AD-A113 542 COLD REGIONS RESEARCH AND ENGINEERING LAB HANOVER NH F/G 8/12
SEA ICE DRAG LAWS AND SIMPLE BOUNDARY LAYER CONCEPTS, INCLUDING--ETC(U)
FEB 82 M G MCPHEE
UNCLASSIFIED CRREL-82-4 NL

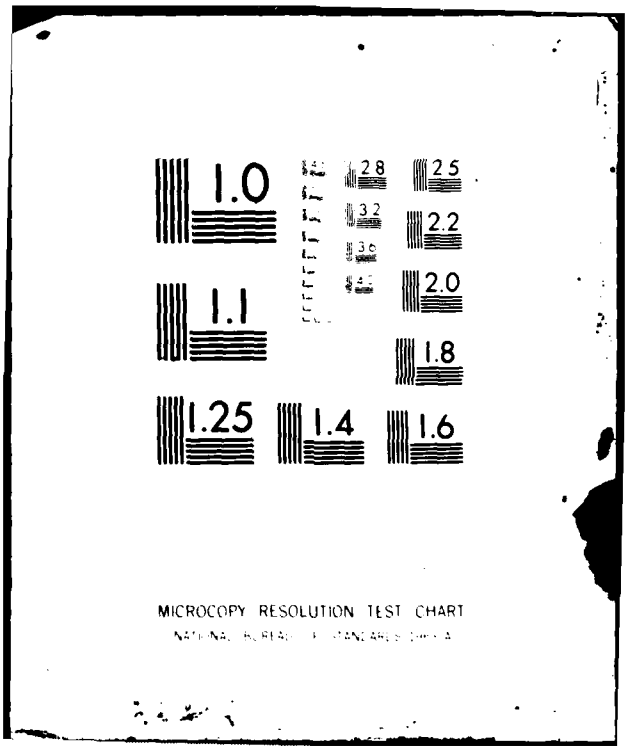
1.0
1.1
1.25
1.4
1.6
1.8
2.0
2.2
2.5
2.8
3.2
3.6
4.0
MICROCOPY RESOLUTION TEST CHART

CRREL REPORT 82-4

13

US Army Corps of Engineers
Cold Regions Research & Engineering Laboratory

Sea ice drag laws and simple boundary layer concepts, including application to rapid melting

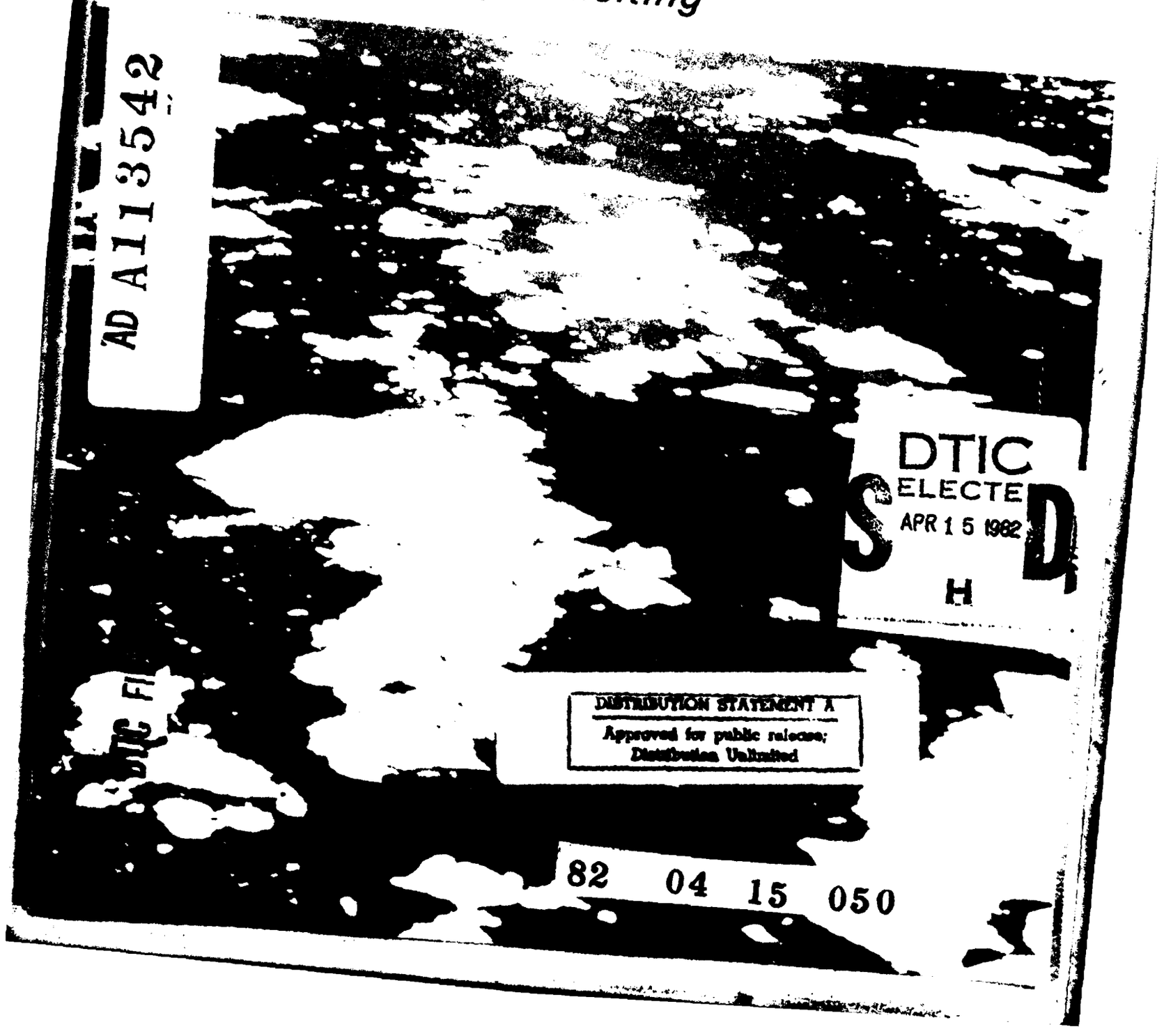

AD A113542

DTIC ELECTE APR 15 1982 S D H

DISTRIBUTION STATEMENT A
Approved for public release;
Distribution Unlimited

82 04 15 050

For conversion of SI metric units to U.S./ British customary units of measurement consult ASTM Standard E380, Metric Practice Guide, *published by the American Society for Testing and Materials, 1916 Race St., Philadelphia, Pa. 19103.*

Cover: Melting ice floes in the Weddell Sea after advection into above-freezing ocean surface water.

CRREL Report 82-4

February 1982

Sea ice drag laws and simple boundary layer concepts, including application to rapid melting

Miles G. McPhee

DTIC
ELECTE
APR 15 1982
S D
H

Prepared for
OFFICE OF NAVAL RESEARCH

Approved for public release; distribution unlimited.

Unclassified

SECURITY CLASSIFICATION OF THIS PAGE (When Data Entered)

REPORT DOCUMENTATION PAGE		READ INSTRUCTIONS BEFORE COMPLETING FORM
1. REPORT NUMBER CRREL Report 82-4	2. GOVT ACCESSION NO. AD-A113 542	3. RECIPIENT'S CATALOG NUMBER
4. TITLE (and Subtitle) SEA ICE DRAG LAWS AND SIMPLE BOUNDARY LAYER CONCEPTS, INCLUDING APPLICATION TO RAPID MELTING		5. TYPE OF REPORT & PERIOD COVERED 6. PERFORMING ORG. REPORT NUMBER
7. AUTHOR(s) Miles G. McPhee		8. CONTRACT OR GRANT NUMBER(s) Office of Naval Research, MIPR N0001480MP00004
9. PERFORMING ORGANIZATION NAME AND ADDRESS U.S. Army Cold Regions Research and Engineering Laboratory Hanover, New Hampshire 03755		10. PROGRAM ELEMENT, PROJECT, TASK AREA & WORK UNIT NUMBERS
11. CONTROLLING OFFICE NAME AND ADDRESS Office of Naval Research Arlington, Virginia 22217		12. REPORT DATE February 1982 13. NUMBER OF PAGES 25
14. MONITORING AGENCY NAME & ADDRESS(if different from Controlling Office)		15. SECURITY CLASS. (of this report) Unclassified 15a. DECLASSIFICATION/DOWNGRADING SCHEDULE

16. DISTRIBUTION STATEMENT (of this Report)

Approved for public release; distribution unlimited.

17. DISTRIBUTION STATEMENT (of the abstract entered in Block 20, if different from Report)

18. SUPPLEMENTARY NOTES

19. KEY WORDS (Continue on reverse side if necessary and identify by block number)

Boundary layer flow	Melting
Drag	Pack ice
Drift	Sea ice

20. ABSTRACT (Continue on reverse side if necessary and identify by block number)

Several proposed methods for treating the momentum flux between drifting sea ice and the underlying ocean are interpreted in terms of simple planetary-boundary-layer (PBL) turbulence theory. The classical two-layer approach, in which the solution for a thin surface layer is matched to an Ekman solution for the outer layer, is used to derive several forms for the drag law. These forms range from linear (where stress is proportional to relative speed), through quadratic (where stress is proportional to relative speed squared), to a Rossby-similarity law like that used to express frictional drag on geostrophic wind in the atmosphere. Only formulations which conform with Rossby-similarity scaling are consistent with free-drift data from the 1975 AIDJEX drift station experiment. We show how a two-layer model, in which the nondimensional stress is allowed to vary realistically through a surface layer of constant nondimensional

DD FORM 1 JAN 73 1473 EDITION OF 1 NOV 65 IS OBSOLETE

Unclassified

SECURITY CLASSIFICATION OF THIS PAGE (When Data Entered)

thickness, provides an analytic solution for the steady-state PBL equation quite similar to recent numerical solutions. The theory is extended to include drag reduction due to buoyancy from rapid melting and is shown to agree with atmospheric results for geostrophic drag under analogous conditions of radiational cooling. The theory provides a basis for estimating trajectories and melt rates of floes drifting into water warmer than the ice melting temperature.

Accession For
NTIS GRA&I ☑
DTIC TAB ☐
Unannounced ☐
Justification
By
Distribution/
Availability Codes
Dist | Avail and/or Special
A

COPY INSPECTED

PREFACE

This report was prepared by Dr. Miles G. McPhee, Geophysicist, of the Snow and Ice Branch, Research Division, U.S. Army Cold Regions Research and Engineering Laboratory. Funding for this research was provided by the Office of Naval Research under MIPR N0001480MP00004, *Analysis of the Physical Oceanographic Data Collected on FRAM I.*

The author thanks Dr. Edgar Andreas and Stephen Ackley of CRREL for technically reviewing the manuscript of this report.

CONTENTS

ILLUSTRATIONS

TABLE

SEA ICE DRAG LAWS AND SIMPLE BOUNDARY LAYER CONCEPTS, INCLUDING APPLICATION TO RAPID MELTING

Miles G. McPhee

BACKGROUND

The drift of sea ice is determined by a balance of forces including a flux of momentum from the ice to the ocean, which is more often than not of the same order of magnitude as the tangential stress exerted on the ice by the wind. Its representation is thus a major element in a mathematical formulation of ice-drift dynamics, and it has received much attention as a problem in planetary-boundary-layer (PBL) theory, beginning with Ekman (1905). Most ice modelers are reluctant to include complete submodels of the oceanic boundary layer in their numerical codes and seek instead to parameterize the tangential stress between the ice and ocean as a function of the ice velocity relative to the undisturbed ocean by using relatively simple expressions which we shall call *oceanic drag laws*. Several drag laws have been proposed by various authors, and a modeler perhaps not well-versed in PBL theory faces the task of choosing a formulation suited to his work. The primary intent of this report is to assist in that choice by providing a framework in which several drag laws may be compared, both in terms of how well they describe pertinent data, and how they fit within the guidelines of PBL theory.

Before the PBL equations could be routinely solved numerically, drag laws for sea ice (and for the atmosphere) were obtained by patching an Ekman-like solution, appropriate for the outer part of the boundary layer, to the solution for a relatively thin layer adjacent to the surface (e.g. Rossby and Montgomery 1935). We shall adopt the same approach, at the same time attempting to rationalize it with recent measurements by progressively introducing concepts from modern turbulence theory into a series of boundary layer formulations which provide drag laws ranging from *linear* (i.e. where stress is proportional to relative speed), through *quadratic* (where stress is proportional to relative speed squared), arriving finally at a Rossby-similarity law consistent with one we proposed earlier on the basis of numerical modeling (McPhee 1979). Most drag laws found in the literature (Shuleikin 1938, Reed and Campbell 1962, Rothrock 1975, McPhee 1975 and 1979, etc.) fall into one of the categories treated.

In addition, the theory is extended to include the effects of rapid melting that might occur if sea ice were advected into comparatively warm water. The problem is addressed both for the practical purpose of interpreting and predicting sea ice behavior near the ice margin and also as a novel application of stable atmospheric boundary layer studies.

Despite the simplicity of the concepts and mathematical models developed here (nearly all the calculations were done with a hand-held calculator—albeit one designed for easy manipulation of complex numbers), the final result is remarkably consistent with the knowledge we have of momentum transfer in a neutral or stably stratified PBL. Thus a second purpose of this report is to emphasize that the ice drift problem can be turned around to reveal much about how boundary layers work. We took this approach, for example, in using ice drift, surface stress, and current meter measurements to corroborate results from a numerical PBL model (McPhee 1979), and also to investigate time-dependent response to rapidly changing winds (McPhee 1980a). Here we bypass some of the more complicated features explored numerically in the earlier works (e.g. inertial waves and abrupt changes in density at the base of the mixed layer) to examine what the stress/velocity relationship for drifting sea ice implies about the basic structure of PBL turbulence.

To start we establish some conventions, the first being that horizontal (two-dimensional) vectors are represented as complex numbers such that $\mathbf{A} = A_x\mathbf{e}_x + A_y\mathbf{e}_y$ (where $\mathbf{e}_x$ and $\mathbf{e}_y$ are orthogonal unit vectors) becomes $\hat{A} = A(\cos\alpha + i\sin\alpha) = Ae^{i\alpha}$, where $i^2 = -1$. The real axis is aligned with $\mathbf{e}_x$, the imaginary axis with $\mathbf{e}_y$, $\alpha = \tan^{-1}(A_y/A_x)$ and $A = |\hat{A}|$. Note that a symbol with a caret indicates a complex (vector)

quantity, while the same symbol without a caret denotes only magnitude. With this convention, it is meaningful to describe products or quotients of vectors, which are also vectors, e.g. for $\hat{B} = Be^{i\beta}$,

$$\hat{A}/\hat{B} = (A/B)e^{i(\alpha-\beta)}.$$

Note also that rotation of a vector in the horizontal plane through an angle θ (positive counterclockwise) occurs if the vector is multiplied by the factor $e^{i\theta}$. Complex notation is introduced both to avoid intricate geometrical constructions and as a computational aid.

The second convention is that, unless otherwise noted, the velocity appropriate for a specific drag law is the relative velocity between the ice and the undisturbed ocean. This relative velocity is the ice velocity with respect to water below the maximum penetration of the frictional PBL, which is also the geostrophic flow due to sea surface tilt (provided there are no horizontal density gradients in the mixed layer). Usually, the ice drift is larger than geostrophic flow and the momentum flux is downward, but the flux direction is unimportant as long as the drag law is expressed in terms of relative velocity.

With complex notation in a frame of reference fixed to earth, the balance of forces acting at a point in a large, uniform slab of ice in steady drift is

$$mf\hat{V}_f e^{i\pi/2} = \rho_a\hat{\tau}_a - \rho_w\hat{\tau}_o + \hat{I} + \hat{S}. \qquad (1)$$

where m = the ice mass per unit surface area
f = the Coriolis parameter
V_f = the absolute ice velocity
ρ_a and ρ_w = air and water densities
$\hat{\tau}_a$ = the kinematic wind stress
$\hat{\tau}_o$ = the kinematic stress exerted by the ice on the ocean
$\hat{I}$ = the force due to a gradient of internal ice stress
$\hat{S}$ = a gravitational force due to sea-surface tilt ($\hat{S} = -mg\nabla\hat{\zeta}$)
ζ = the elevation of the sea surface
g = the acceleration of gravity.

By definition, geostrophic flow in the ocean V_g is given by

$$f\hat{V}_g e^{i\pi/2} = -g\nabla\hat{\zeta} = \hat{S}/m \qquad (2)$$

so that

$$mf(\hat{V}_f - \hat{V}_g)e^{i\pi/2} = imf\hat{V} = \rho_a\hat{\tau}_a - \rho_w\hat{\tau}_o + \hat{I}$$

where $\hat{V}$ is the relative velocity described above.

In McPhee (1979) we analyzed the relationship between $\hat{\tau}_w$ and $\hat{V}$, using wind stress and drift velocity measured during the 1975 summer melt season at four drifting stations of the AIDJEX Experiment near the center of the Beaufort Gyre in the central Arctic. The major difference between this and earlier analyses (the most extensive being that of Reed and Campbell 1962) is that we considered only data from a 60-day period during which we were reasonably confident that the internal ice force $\hat{I}$ was small. During the remainder of the year-long AIDJEX drift, $\hat{I}$ was often a significant part of the force balance (McPhee 1980b), and affected the long-term statistics of ice drift appreciably. During the short time of the year when $\hat{I}$ is negligible, measurements of V_f and the 10-m wind velocity, $\hat{U}_{10}$, along with estimates of $\hat{V}_g$, m, and the wind drag coefficient, C_{10}, provide the interfacial stress $\hat{\tau}_o$ from the relation

$$\rho_w\hat{\tau}_o = \rho_a C_{10}U_{10}\hat{U}_{10} - imf\hat{V}. \qquad (3)$$

Given a sufficient population of sample pairs, τ_o and V, an expression of the form

$$\tau_o = aV^b$$

can be derived statistically by a linear regression of the equation

$$\log\tau_o = b\log V + \log a.$$

Figure 1 from McPhee (1979) shows results of such an analysis on summer AIDJEX data filtered to

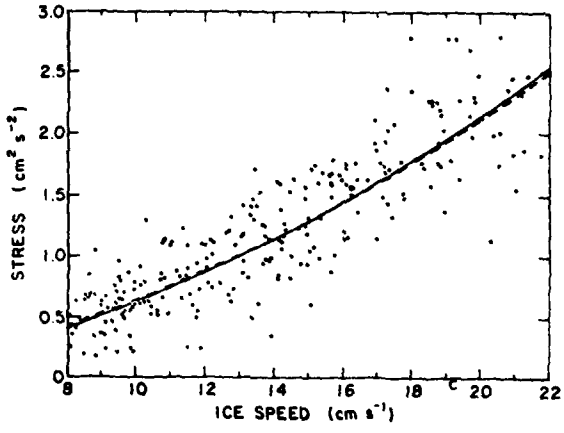

Figure 1. Kinematic stress vs relative speed between ice and ocean under free-drift conditions. Solid curve is best-fit exponential, dashed curve is theoretical prediction from McPhee (1979).

remove inertial motion. In all, 254 samples were obtained with relative speeds greater than 8 cm s^{-1} (in order to minimize the effect of uncertainty in $\vec{V}_g$). Stress was calculated for each sample according to eq 3 with $C_{10} = 0.0027$ and $m = 250$ g cm^{-2}. By least-squares regression, the exponent b with a 90% confidence interval, was found to be 1.78 ± 0.12. Thus the relationship was close to quadratic ($b = 2$), but statistically different at the 90% confidence level.

The calculated magnitudes of a and the deflection angle β between $\vec{\tau}_o$ and $\vec{V}$, are sensitive to C_{10} and m, both of which have relatively large uncertainties. However, we showed (McPhee 1979, Table 1) that the exponent b is insensitive to variation in C_{10} and m over a large range of plausible values. We therefore concluded that, despite uncertainties in stress magnitude and β, the *shape* of the τ_o vs V curve as indicated by b was well-defined by the data, and that a proper stress formulation should exhibit similar shape. The dashed curve in Figure 1 results from the numerical model of McPhee (1979): its shape factor turned out to be $b = 1.70 \pm 0.00$, which was within the confidence interval found for the data.

It was more difficult to assign an experimental value to β. One measure was the angle between negative ice drift and current velocity measured at 0.2-m depth. Over the entire year, the average for all camps was about 24° (McPhee 1980b, Table 2) but there was much scatter in the data. Precise current measurements from the 1972 AIDJEX Pilot Study also showed β to be about 24°, so this value was accepted for an average, but with much less certainty than the value for b.

In the next section, we consider several drag laws, each with a corresponding simple PBL model. Our evaluation of each law depends primarily on how well it satisfies the shape requirements implied by the AIDJEX data.

HIERARCHY OF DRAG LAWS AND SIMPLE MODELS

The drag law in complex notation

In order to simplify as much as possible a comparison among several drag formulations, it is useful to express the drag law, as follows. First define the friction velocity as

$$\vec{u}_* \equiv \frac{\vec{\tau}_o}{\tau_o^{1/2}} .$$

where $\vec{\tau}$ is the vector kinematic stress at the interfaces. Note that $\vec{u}_*$ is a vector (complex number) in the direction of $\vec{\tau}_o$ with magnitude $\tau_o^{1/2}$.

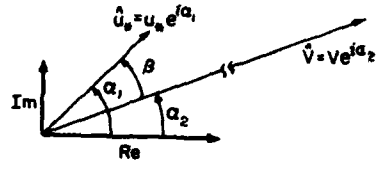

Figure 2. Schematic of friction velocity/surface velocity relation in complex plane.

From comments in the previous section, we expect realistic drag laws to fall closer to *quadratic* (i.e. $\tau_o \propto V^2$) than *linear* ($\tau_o \propto V$) and to exhibit a turning angle of the order of 20° to 30°. Using complex notation, we express the drag law as a ratio of $\vec{V}$ and $\vec{u}_*$:

$$\frac{\vec{V}}{\vec{u}_*} = \vec{\Gamma} = \Gamma e^{-i\beta} . \qquad (4)$$

From Figure 2 we have

$$\vec{\Gamma} = \frac{\vec{V}}{\vec{u}_*} = \frac{V}{u_*} e^{i(\alpha_1 - \alpha_2)}$$

so that $\Gamma = V/u_*$ is a dimensionless surface speed and $\beta = \alpha_2 - \alpha_1$ is the rightward (f positive) deflection angle of surface velocity with respect to interfacial stress. Note that Γ and β are constant for quadratic drag with constant turning angle; all other laws have Γ and β dependent on other parameters of the problem (e.g. u_*, f, etc.). Expressing the drag law as a complex ratio greatly simplifies its algebraic representation and is computationally useful (e.g. given u_*, $\vec{V}$ is found by a scaling, Γ, and rotation, $e^{-i\beta}$).

The momentum equation for the planetary boundary layer

The horizontally homogeneous, steady-state PBL equation of motion is given in complex notation by

$$if\vec{U}_f = if\vec{V}_g + \frac{\partial \vec{\tau}}{\partial z} \qquad (5)$$

where $\vec{U}_f$ is the velocity in a frame of reference fixed to earth, $\vec{\tau}$ is the kinematic, turbulent Reynolds stress, and we have expressed the pressure gradient due to sea-surface tilt in terms of the geostrophic velocity from eq 2. As with the ice momentum equation, we eliminate $\vec{V}_g$ by considering a reference frame drifting with the geostrophic velocity; hence for $\vec{V} = \vec{U}_f - \vec{V}_g$, eq 5 becomes

$$if\ \vec{V} = \frac{\partial \vec{\tau}}{\partial z}. \qquad (6)$$

To solve eq 6 an expression for $\vec{\tau}$ is required and here we make the simplest closure assumption, i.e. that stress is related to $\partial \vec{U}/\partial z$ by an eddy viscosity coefficient:

$$\vec{\tau} = K_m \frac{\partial \vec{U}}{\partial z}$$

Thus eq 6 becomes

$$if\ \vec{U} = \frac{\partial}{\partial z}\left(K_m \frac{\partial \vec{U}}{\partial z}\right). \qquad (7)$$

In the remainder of this section we show how various drag laws imply a variety of simple formulations for the eddy viscosity.

Eddy viscosity

The essential tenets of the eddy viscosity concept are that turbulent transfer (overturning associated with instabilities in the flow field) is much more efficient than molecular transfer, and that, in some way, this turbulent transfer can be expressed in terms of mean properties of the flow. Note the fundamental distinction between properties of the flow and properties of the fluid, as emphasized, for example, by Tennekes and Lumley (1972, Chapter 1).

Figure 3 depicts an overturning eddy in a fluid characterized by a gradient of some property, ϵ. A conspicuous feature of turbulence (as opposed, say, to organized waves) is its highly diffusive nature; fluid parcels caught up in a turbulent eddy, as shown, become involved in progressively smaller eddies and readily transfer their properties to the surrounding fluid. In Figure 3 parcel 1 distributes a deficit of ϵ to the flow above h, and parcel 2 distributes an excess below h, so that a downward flux of ϵ across the surface $z = h$ occurs. This flux apparently depends on three quantities: first, the gradient of the property $d\epsilon/dz$, second, the overturning velocity v, and finally the length scale ℓ of the most energetic eddies found in that particular region of the flow.

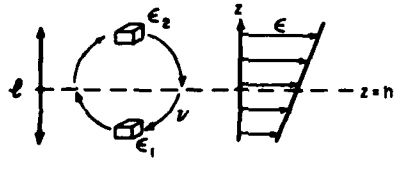

Figure 3. Diagram of turbulent flux mechanism.

The last is not necessarily obvious, because turbulence comprises a broad spectrum of length scales. The interpretation here is that ℓ is the scale of the largest eddies with which smaller eddies can "keep up," i.e. diffuse the property to the surrounding fluid. Note that for different properties in the same flow, ℓ may have different values.

The simplest expression for the flux of ϵ across the horizontal surface is linear in each quantity, viz

$$F_\epsilon = -v\ell_\epsilon \frac{d\epsilon}{dz}.$$

By analogy with molecular diffusivity, we may define an "eddy diffusivity" $K_\epsilon = v\ell_\epsilon$ with units L^2T^{-1} such that

$$F_\epsilon = -K_\epsilon \frac{d\epsilon}{dz}.$$

If the property in question is momentum, then the vertical momentum flux, which is minus the horizontal part of the turbulent stress tensor and therefore a vector, is given by

$$\vec{F}_m = -\rho\vec{\tau} = -\rho K_m \frac{\partial \vec{U}}{\partial z} \qquad (8)$$

where $\vec{U}$ is the mean velocity vector and $\vec{\tau} = -(\overline{u'w'} + i\overline{v'w'})$ is the Reynolds stress.

Linear drag – constant eddy viscosity

The simplest solution to the PBL momentum equation is obtained when K_m has no depth dependence (Ekman 1905). With the further stipulation that K_m is independent of other variables, the solution provides a linear drag law. Equation 7 becomes

$$if\ \vec{U} = K_m \frac{\partial^2 \vec{U}}{\partial z^2}$$

with solution

$$\vec{U} = \vec{A}e^{\vec{\delta}z} + \vec{B}e^{-\vec{\delta}z}$$

$$\vec{\delta} = \left(\frac{if}{K_m}\right)^{1/2} = (f/K_m)^{1/2} e^{i\pi/4}$$

$$= (f/2K_m)^{1/2}(1+i)$$

As $\vec{U}$ is bounded at depth ($z \to -\infty$), $\vec{B} = 0$; therefore

$$\vec{U}(z) = \vec{V}_E e^{\vec{\delta}z} = \vec{V}_E e^{(f/2K_m)^{1/2}z} \times e^{i(f/2K_m)^{1/2}z} \qquad (9)$$

where $\vec{V}_E$ is the surface Ekman velocity.

Since δ is complex, the solution has both oscillatory and exponentially decaying components in z, providing the well-known Ekman spiral in which the drift current rotates and decreases with depth. Note that δ is the inverse of an "e-folding" PBL depth scale which varies as $(K_m/f)^{1/2}$.

Our specific interest is the relation between surface stress and velocity, given by the boundary condition

$$\vec{\tau}_o = u_* \vec{u}_* = K_m \left.\frac{\partial \vec{U}}{\partial z}\right|_{z=0}$$

$$= (fK_m)^{1/2} \vec{V}_E e^{i\pi/4} .$$

The drag law for the Ekman solution is thus

$$\frac{\vec{V}_E}{\vec{u}_*} = (fK_m)^{-1/2} u_* e^{-i\pi/4} \qquad (10)$$

i.e. $\Gamma = u_*/(fK_m)^{1/2}, \beta = 45°$.

If K_m is constant with respect to all variables, drawbacks are immediately apparent. First, drift data show that the drag law is *not linear, and that* β is about half 45°. From the viewpoint of simple turbulence theory, K_m being constant implies that the product of mixing length and turbulent velocity is a property of the fluid. Instead, we intuitively expect larger, more energetic eddies (ℓ and v both increasing) as the ice speed increases.

Despite its shortcomings, the so-called Ekman approach has often been used for ice modeling because the stress is linear in V. Some authors have reduced the turning angle to values closer to those observed. For example, Rothrock (1975) used a linear drag law of the form

$$\frac{\vec{V}}{\vec{u}_*} = (fK_R)^{-1/2} u_* e^{-i\beta} \qquad (11)$$

where $\beta = 20°$ and $K_R = 24$ cm^2 s^{-1}, following the value for eddy viscosity under sea ice reported by Hunkins (1966).

To be consistent with Ekman theory, reducing the drift angle is tantamount to inserting a layer with constant stress between the ice and the Ekman layer. If this layer is thin enough, the change in stress across it will be small, yet there will be a considerable current shear in the direction of stress. The concept is sketched in Figure 4, and we shall analyze the problem in some detail to establish a pattern for subsequent refinements.

$\vec{V}$ is the vector sum of $\vec{V}_E$ and $\vec{V}_s$, the latter being the velocity of the surface with respect to the average velocity at the level $z = -h$. Integration of eq 8 for constant K_m and stress yields

$$\frac{\vec{V}_s}{\vec{u}_*} = \frac{u_* h}{K_m} \qquad (12)$$

where h is the depth of the constant stress layer. Note that this complex ratio has no imaginary component: $\vec{V}_s$ is in the same direction as u_*. The stress acting at the top of the Ekman layer, $z = -h$, is assumed unchanged, so the drag law is obtained by combining eq 10 and 11:

$$\vec{\Gamma} = \frac{\vec{V}}{\vec{u}_*} = (2fK_m)^{-1/2} u_*$$

$$\times [1 + h(2f/K_m)^{1/2} - i] . \qquad (13)$$

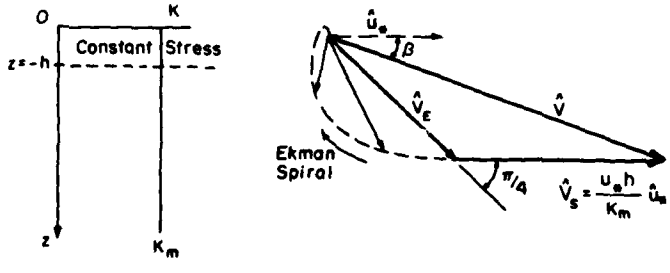

Figure 4. Two-layer system with constant eddy viscosity. Note that shear in the surface layer is constant. The actual current rotates clockwise with increasing depth in both layers.

Since β is specified, the relation

$$\tan\beta = \frac{-Im(\hat{\Gamma})}{Re(\hat{\Gamma})} = [1 + h(2f/K_m)^{1/2}]^{-1} \quad (14)$$

determines h and (eq 13) may be rewritten as

$$\hat{\Gamma} = \frac{\hat{V}}{u_*} = (2f/K_m)^{-1/2} \csc\beta\, u_* e^{-i\beta} \quad (15)$$

Note that the eddy viscosity in the Ekman layer is related to that specified in eq 11 by

$$K_m = K_R \csc^2\beta/2$$

which for Rothrock's value (24 $cm^2\ s^{-1}$) provides a "real" eddy viscosity about four times that reported by Hunkins. Solving eq 14 for h with $\beta = 20°$ yields a thickness of about 10 m for the surface layer, which is, of course, unrealistically large for the assumption of constant stress. This exercise, in which the linear drag law is interpreted in terms of an Ekman layer overlain by a constant-stress layer, demonstrates that such laws have little basis in PBL theory, although they are sometimes justified by Hunkins' (1966) eddy-viscosity estimate. It is worth noting in this regard that Ekman (1905) treated eddy viscosity as constant only in the sense of having no vertical variation. In fact, he postulated, with characteristic insight, that in the open sea eddy viscosity should vary as the square of the surface wind, a view corroborated by the present results.

Linear eddy viscosity – the constant stress layer

Near a solid surface in a developed turbulent flow, eddy momentum flux is comparatively well understood. Much experimental evidence indicates that the proper velocity and length scales in the eddy viscosity expression are $\nu = u_*$ and $\ell = k|z|$ where k is von Karman's constant, $k = 0.4$. Integration of eq 8 for constant stress between levels $z = -h$ and $z = -z_o$ yields the familiar law of the wall:

$$\hat{V}_s = \hat{U}(-z_o) - \hat{U}(-h) = \frac{1}{k} \ln\left(\frac{h}{z_o}\right) \hat{u}_* \,. \quad (16)$$

The surface roughness length z_o represents a scale at which protrusions on the ice underside are sensed by the turbulent flow. For a surface with nonuniform relief like an ice floe, it is hard to assign a precise physical meaning to z_o; we take it to be the level at which mean turbulent stress equals the overall interfacial stress, and above which there is no *mean* shear in the water column, averaged spatially.

For fixed h, eq 16 is a quadratic drag with no turning, but the constant stress approximation and the required alignment of stress and relative current clearly restrict its region of validity to values of h that are small compared to the total PBL depth, so that V_s is never equal to V.

Two-layer eddy viscosity

Figure 5 depicts a boundary layer in which eddy viscosity increases linearly until it reaches a maximum at some level $z = -h$, below which it is constant. If the stress at $z = -h$ is not much changed from the surface value, the water column below h will form an Ekman spiral as if driven by the interfacial stress. Between the ice and $z = -h$ there is a logarithmic velocity profile in the direction of $\hat{u}_*$. As before, the surface velocity $\hat{V}$ is the sum of $\hat{V}_E$ and $\hat{V}_s$, both known functions of $\hat{u}_*$.

Because there is no physical change in the fluid at $z = -h$, we assume that the mixing length is continuous across the transition. This still allows considerable freedom in prescribing the flow. For example, we might again specify that K_m is independent of all other variables, in which case $h = K_m/u_*$. So by combining eq 10 and 16, we have

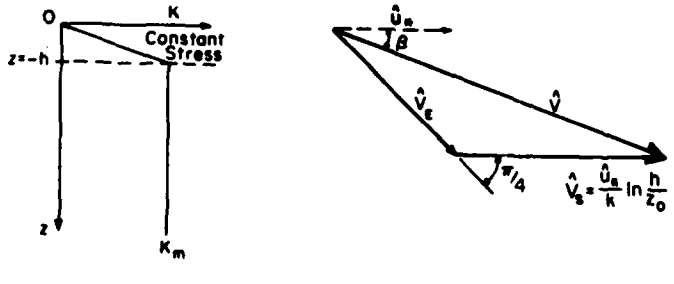

Figure 5. Two-layer system with linear eddy viscosity near surface. Shear in the surface layer varies inversely as depth, causing logarithmic current profile from z = -h to surface.

$$\Gamma = \frac{\dot{V}}{\dot{u}_*} = (2fK_m)^{-1/2}\, u_* \left[1 + \frac{(2fK_m)^{1/2}}{ku_*} \times \ln\left(\frac{K_m}{ku_* z_o}\right) - i \right] . \qquad (17)$$

A problem is immediately apparent here because as u_* increases, the constant stress layer becomes thinner. The maximum size of eddies generated within the surface layer ($|z| < h$) thus decreases with increasing stress, so that the drag law approaches the constant Ekman solution at higher speeds. All of this is contrary to our physical reasoning.

Reed and Campbell (1962) developed a more realistic approach by specifying a constant value for h and then matching the magnitude of the eddy viscosity in the Ekman layer to the surface-layer value at $z = -h$. In effect they postulated a physical limitation on the maximum effective eddy size (mixing length) rather than on the eddy viscosity. Hence $K_m = ku_*h$ where h is an assigned constant and the Reed-Campbell drag law (with the simplification $z_o + h \approx h$) is

$$\Gamma = \frac{\dot{V}}{\dot{u}_*} = \left(\frac{u_*}{2fkh}\right)^{1/2} \left\{ 1 + \left(\frac{2fh}{ku_*}\right)^{1/2} \times \ln\left(\frac{h}{z_o}\right) - i \right\} \qquad (18)$$

so that

$$\beta = \cot^{-1}\left\{ 1 + \left(\frac{2fh}{ku_*}\right)^{1/2} \ln\left(\frac{h}{z_o}\right) \right\}$$

$$\Gamma = u_*^{1/2}\, (2fkh)^{-1/2}\, \csc\beta .$$

The Reed-Campbell formulation recognizes that eddy viscosity in the outer layer depends on surface stress, but there is still an important conceptual stumbling block: why should h be the same for a flow with low turbulence levels (small u_*) as for a flow having high turbulence levels? We might instead expect the maximum mixing length to depend on other flow parameters as well.

PBL scaling

Rossby (1932) and Rossby and Montgomery (1935) were apparently the first to explore the idea that the maximum eddy viscosity for the rotational PBL is proportional to a velocity scale times a length scale which appears from dimensional analysis of the momentum equation; namely, the velocity scale divided by the Coriolis parameter f (they used the geostrophic wind speed in the atmosphere, analogous to V here). Much subsequent work for the atmospheric PBL has relied heavily on this idea except that the commonly used scales are u_* and u_*/f for velocity and length (there is a subtle difference because u_* and V are not exactly proportional). The basic idea is that turbulent boundary layers in rotating flows are dynamically similar in regions suitably far away from solid surfaces, provided density is uniform and flow variables are scaled by u_*^2, u_*, and u_*/f for kinematic stress, velocity, and length respectively.

Although this framework has proved a powerful tool for classifying and modeling the atmospheric PBL, it has not been as widely accepted for oceanic modeling (see, for example, Kraus 1977). Whatever the reasons for this, the results from under-ice studies of PBL mean flow and turbulence during the AIDJEX experiments strongly support Rossby-type scaling (McPhee and Smith 1976, McPhee 1979 and 1980a). Of special significance are measurements of turbulent stress and turbulent energy spectra reported by McPhee and Smith (1976). We found that atmospheric models adequately described our turbulence data when scaled as above. Furthermore, we used peaks in the spectra of vertical velocity fluctuations at several levels through the PBL to show that a dimensionless eddy viscosity distribution (fK_m/u_*^2) increased more or less linearly with distance from the surface until it reached a maximum at a depth some fraction of the total PBL depth, beyond which it decreased slowly. While this is not the simple two-layer system discussed here, we found (McPhee 1979) that there was little difference between numerical solutions of the PBL equations using an exponentially attenuated linear eddy viscosity (similar to the observed regime) and a linear-constant two-layer system (compare Fig. 1 and 2 of McPhee 1979). This observation, in fact, prompted the present work.

Why turbulent eddies should be limited in size by rotational effects (i.e. that the maximum mixing length should be proportional to u_*/f) is addressed in some detail by Stern (1975, Chapter 8). From a stability analysis of the PBL equation, he shows that energy is spontaneously radiated downward in inertial waves if the scale of turbulent fluctuations exceeds a length proportional to u_*/f. He concludes that this provides an effective "brake" on surface-driven turbulence which tends to keep the scale of the largest disturbances near this instability-governed limit.

A dimensionless two-layer system

The ideas above can be easily incorporated into the two-layer model as sketched in Figure 6. All

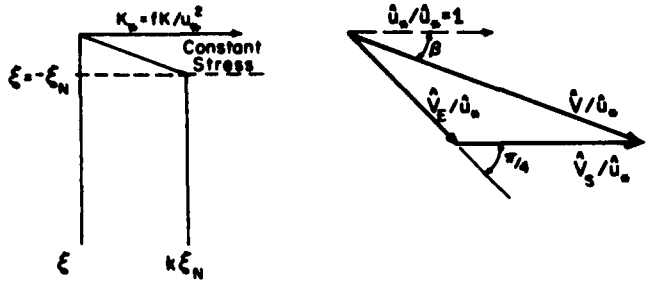

Figure 6. Two-layer system nondimensionalized by Rossby-similarity scales. Note that actual eddy viscosity in Ekman layer is proportional to u_*^2/f.

quantities are nondimensionalized and we assume that there is a "universal" maximum nondimensional mixing length ξ_N. The outer layer eddy viscosity is then

$$K_m = k\xi_N u_*^2/f$$

and the Ekman solution (eq 10) is

$$\frac{\dot{V}_E}{\dot{u}_*} = (k\xi_N)^{-1/2}\, e^{-i\pi/4}$$

which is clearly a quadratic drag law. The surface layer solution is

$$\frac{\dot{V}_s}{\dot{u}_*} = \frac{1}{k}\ln\left(\frac{\xi_N}{\xi_o}\right)$$

where $\xi_o = fz_o/u_*$ is the "nondimensional roughness length." The drag law for the combined system is

$$\dot{\Gamma} = \frac{\dot{V}}{\dot{u}_*} = (2k\xi_N)^{-1/2}\left\{1 + \left(\frac{2\xi_N}{k}\right)^{1/2} \times \ln\left(\frac{\xi_N}{\xi_o}\right) - i\right\} \qquad (19)$$

and

$$\beta = \cot^{-1}\left\{1 + \left(\frac{2\xi_N}{k}\right)^{1/2} \ln\left(\frac{\xi_N}{\xi_o}\right)\right\} \qquad (20)$$

$$\Gamma = (2k\xi_N)^{-1/2}\csc\beta\,. \qquad (21)$$

Equation 19 reduces to a pure quadratic drag law if ξ_o is constant. This stipulation is questionable, because unlike the turbulence scales in the outer layer, z_o is a physical property of the surface itself, and there is no a priori reason to assume it scales with u_*/f. In formulating the drag law for the AIDJEX Model (McPhee 1975), we assumed that over the limited range of u_*/f encountered during meaningful simulations, the effect of variations in the "surface-friction Rossby number" ($Ro_* = u_*/fz_o = 1/\xi_o$) would be minor and that a quadratic drag law would suffice. This was in part due to uncertainty about a suitable value for z_o, since it represents an aggregate roughness over perhaps several large floes. The success of subsequent simulation of summer drift using the quadratic drag (McPhee 1980b) tended to reinforce this view.

On the other hand, analysis of drift statistics described previously indicated that the drag law is slightly different from quadratic, so we might rather treat z_o as constant, which gives both β and Γ slight dependence on u_*/f through the term $\ln(\xi_N/\xi_o)$ in eq 20. The two-layer system of eq 19 with z_o constant includes most of the features required for a conceptual model in which the size of momentum exchanging eddies increases as the distance from the interface, but is limited to some fraction of u_*/f by an instability mechanism which rapidly propagates energy away from the boundary layer once the size limit is exceeded. All such flows, when scaled as above, are similar except in a thin region right next to the interface in which the other physical length scale z_o asserts itself.

As an historical note, Ekman (1905) assumed that the depth of frictional influence [$D = \pi(2K_m/f)^{1/2}$] in the open ocean varied as $W/(\sin\phi)^{1/2}$ where W is the surface wind velocity and ϕ is latitude. We see that, if the dependence were rather $D \propto W/\sin\phi$

(proportional to u_*/f), this would provide an eddy viscosity such that fK_m/u_*^2 is constant (rather than K_m), resulting in a quadratic drag. If the minor variation of f at high latitudes is ignored, faithful application of Ekman's ideas does result in a quadratic drag, and the turning angle becomes realistic when a surface layer such as that of Shuleikin (1938) is provided.

While the modeling results of McPhee (1979) showed that the particular shape of the nondimensional eddy viscosity distribution in the outer layer is not overly important, there remains an obvious question about the two-layer approach: specifically, how valid is the assumption of constant stress in the surface layer? Here the numerical results are less encouraging: they show that at the level $\xi = -\xi_N$, the nondimensional stress has decreased in magnitude by about 20% and rotated clockwise perhaps 20° from its surface value (see Fig. 2 of McPhee 1979). This suggests a final modification to the two-layer system.

A dimensionless two-layer system with modified stress

Equation 6, nondimensionalized, has the form

$$\hat{u} = \frac{\partial \hat{T}}{\partial \xi} \tag{22}$$

where $\xi = fz/u_*$, $\hat{u} = \bar{U}/\hat{u}_*$, and $\hat{T} = \bar{\tau}/u_*\hat{u}_*$. The nondimensional stress at ξ is thus

$$\hat{T}(\xi) = \hat{T}_o - i\int_{\xi}^{-\xi_o} u\,d\xi \tag{23}$$

where the subscript o denotes the surface values. To find $\hat{T}_E = \hat{T}(-\xi_N)$, we first note that $\hat{T}$ is aligned at the surface with the real axis (i.e. $\hat{T}_o = 1$), and then assume that within the surface layer ($|\xi| < \xi_N$) shear in the lateral (imaginary) component of velocity is negligible. Since the real part of the surface-layer velocity varies logarithmically, integration of eq 23, evaluated with the approximation $\xi_N + \xi_o \cong \xi_N$, yields

$$\hat{T}_E = 1 - i(\hat{v}_E + 1/k)\,\xi_N \tag{24}$$

where $\hat{v}_E = \hat{u}(-\xi_N)$ is the nondimensional Ekman velocity forced by the attenuated and rotated surface stress $\hat{T}_E$. Using this as the upper boundary condition in the nondimensional Ekman solution we have

$$\hat{v}_E = \frac{\hat{V}_E}{\hat{u}_*} = (k\xi_N)^{1/2}\,\hat{T}_E\,e^{-i\pi/4} \tag{25}$$

and substituting into eq 24

$$\hat{T}_E = (1 - i\xi_N/k)/[1 + (\xi_N/2k)^{1/2}(1+i)]$$

$$= 1 - (\xi_N/2k)^{1/2}(1+i)\,. \tag{26}$$

For the value $\xi_N = 0.045$, derived in the next subsection, we have $T_E = 0.80$, $\theta = -17.3°$, which agrees well with the numerical result of McPhee (1979).

Solving for v_E from eq 24, we have

$$\hat{v}_E = (2k\xi_N)^{1/2}(1-i) - 1/k$$

$$\hat{\Gamma} = \frac{\hat{V}}{\hat{u}_*} = (2k\xi_N)^{-1/2}\left\{1 + (2\xi_N/k)^{1/2} \times [\ln(\xi_N/\xi_o) - 1] - i\right\} \tag{27}$$

and the system is sketched in Figure 7.

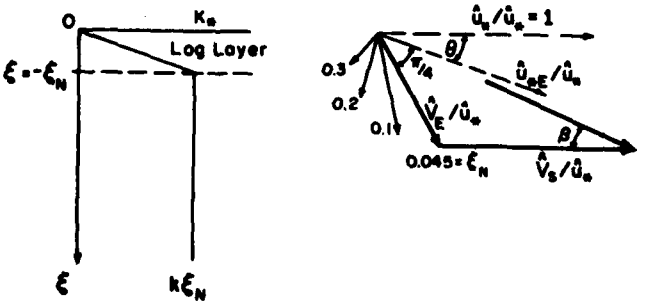

Figure 7. Two-layer system in which stress is allowed to vary through a logarithmic surface layer. The direction and relative magnitude of the friction velocity at the top of the Ekman layer is indicated by $\hat{u}_{*g}$. Numbers beside current vectors denote nondimensional depth units, $-fz/u_*$.

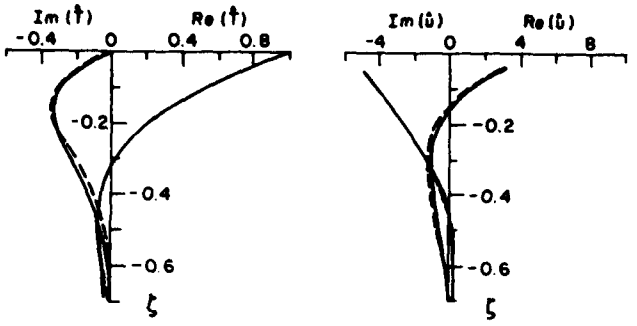

Figure 8. Nondimensional stress and velocity in the planetary boundary layer according to two-layer model with modified stress (solid curves) and atmospheric PBL model of Businger and Arya (1974) (dashed curves). Velocity provile in the surface layer ($|\xi_N| < 0.045$) depends on z_o.

In addition to the drag law, this approach allows a complete specification of velocity and stress throughout the boundary layer. The Ekman solution for the outer layer is

$$\hat{u}(\xi) = \hat{v}_E \, e^{\hat{\eta}(\xi + \xi_N)}, \quad \xi < -\xi_N \tag{28}$$

where $\hat{\eta} = u_* \hat{\delta}/f = (2k\xi_N)^{-1/2}(1 + i)$. For the surface layer,

$$\hat{u}(\xi) = \hat{v}_E + \frac{1}{k} \ln(\xi_N/|\xi|),$$

$$\xi_o << |\xi| < \xi_N . \tag{29}$$

The nondimensional stress, $\hat{T} = \hat{\tau}/u_* \hat{u}_*$, is, for the outer layer,

$$\hat{T}(\xi) = \hat{T}_E \, e^{\hat{\eta}(\xi + \xi_N)}, \quad \xi < -\xi_N \tag{30}$$

and for the surface layer the stress is well approximated by

$$\hat{T}(\xi) = 1 + i(\hat{v}_E + 1/k)\xi,$$

$$\xi_o << |\xi| < \xi_N . \tag{31}$$

Equations 28-31 constitute a closed PBL model for the neutral boundary layer unaffected by a pycnocline. Solutions for $\xi < -\xi_N$ (= 0.045) are drawn in Figure 8 along with results for the neutrally stable atmospheric PBL from the numerical model of Businger and Arya (1974). The agreement is remarkable considering that the only adjustable parameter in the analytic solution, ξ_N, was chosen by comparing the drift of sea ice with the stress exerted upon it by the wind.

Evaluating the drag laws

From the concept of a surface layer separating the ice-ocean interface from a pure Ekman layer, we have constructed a sequence of six drag laws, each one hopefully including a slightly more sophisticated view of the boundary-layer structure than the one before it. Most expressions for water stress used in ice modeling fit into one of these categories:

1. Constant eddy viscosity, reduced turning angle (eq 13).
2. Logarithmic, constant-stress surface layer, constant eddy viscosity (eq 17).
3. Reed-Campbell approach, h constant (eq 18).
4. Nondimensional eddy viscosity, constant β (eq 19, ξ_o constant).
5. Rossby similarity scaling, constant-stress surface layer (eq 19, z_o constant.
6. Rossby similarity scaling, logarithmic surface layer with modified stress (eq 27).

In order to compare the drag laws among themselves and with the AIDJEX free-drift data, values for the pertinent parameters in each expression were chosen so that when u_* is equal to 1 cm s^{-1}, $\Gamma = 13$ and $\beta = 24°$. The value for Γ comes from the fitted τ vs V curve (Fig. 1) evaluated at $u_* = 1$ cm s^{-1}, which was close to the average condition encountered during the 1975 melt season. Expressions for β and Γ are summarized in Table 1

Table 1. Summary of drag laws.

*Drag law**	β	Γ	*Parameters*	*Stress-speed equation*
1	24°	$(2fK_m)^{-1/2} \csc \beta u_*$	$K_m = 128\ \text{cm}^2\ \text{s}^{-1}$	$\tau = 0.077V$
2	$\cot^{-1}\left\{1 + \frac{(2fK_m)^{1/2}}{ku_*} \ln\left(\frac{K_m}{ku_* z_o}\right)\right\}$	$(2fK_m)^{-1/2} \csc \beta u_*$	$K_m = 128\ \text{cm}^2\ \text{s}^{-1}$ $z_o = 23$ cm	$\tau = 0.023V^{(1.46\pm0.02)}$
3	$\cot^{-1}\left\{1 + \left(\frac{2fh}{ku_*}\right)^{1/2} \ln\frac{h}{z_o}\right\}$	$(2fkh)^{-1/2} \csc \beta u_*^{1/2}$	$h = 319$ cm $z_o = 23$ cm	$\tau = 0.0177V^{(1.57\pm0.00)}$
4	24°	13		$\tau = 0.0059V^2$
5	$\cot^{-1}\left\{1 + \left(\frac{2\xi_N}{k}\right)^{1/2} \ln\left(\frac{\xi_N u_*}{fz_o}\right)\right\}$	$(2k\xi_N)^{-1/2} \csc \beta$	$\xi_N = 0.045$ $z_o = 23$ cm	$\tau = 0.0128V^{(1.70\pm0.00)}$
6	$\cot^{-1}\left\{1 + \left(\frac{2\xi_N}{k}\right)^{1/2} \left[\ln\left(\frac{\xi_N u_*}{fz_o}\right) - 1\right]\right\}$	$(2k\xi_N)^{-1/2} \csc \beta$	$\xi_N = 0.045$ $z_o = 8.5$ m	$\tau = 0.0128V^{(1.70\pm0.00)}$

* $\frac{\hat{V}}{\hat{u}_*} = \Gamma e^{-i\beta}$

for each model. Note that no attempt was made to choose "physically realistic" parameters garnered from the literature. Our reasoning was that the laws were best compared by having them all agree at one point within the range of acceptable data.

Curves coinciding with the chosen parameters are plotted in Figure 9 along with the envelope of the experimentally determined exponent, $b = 1.78 \pm 0.12$. In addition, these curves were fitted to the stress relation

$$\tau = aV^b$$

with a least-squares analysis of the 29 points used to generate each curve. Values of b with 90% confidence brackets are tabulated for each of the drag laws in the last column of Table 1. Only laws 5 and 6 fall within the 90% error bounds of the observed data. The stress-speed relationship is thus best described by the Rossby-similarity laws, which include the most extensive treatment of the principles governing turbulent flow. Note that, although the drag results are very similar for both Rossby-similarity approaches, the effective surface roughness is smaller in the reduced stress model (eq 27), falling close to the value (10 cm) determined in McPhee (1979). As we have shown, the two-layer model with reduced stress is a close approximation of the numerical results of Businger and Ayra (1974) and McPhee (1979) for determining stress and velocity at all levels in the boundary layer. In flows where a shallow pycnocline occurs, flow profiles are affected at lower levels and drag characteristics are apparently changed slightly as discussed in McPhee (1979). We reiterate that when the ice pack is weak enough to admit inertial oscillation, the drag laws here are appropriate only for motion averaged for time scales of the same order or longer than the inertial period (~ 12 hours).

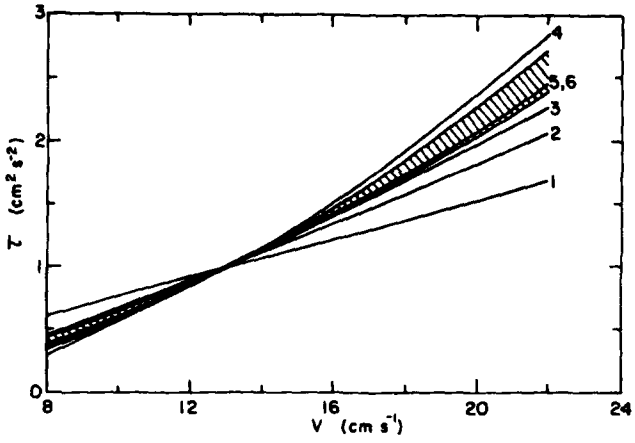

Figure 9. Comparison of six drag law formations with data from 1975 AIDJEX Experiment. Shaded portion shows the limits of the empirical fit included in the 90% confidence interval.

Rossby similarity parameters and buoyancy effects

The usual approach to parameterizing surface drag on the atmospheric free stream using Rossby-similarity scaling is somewhat different from that developed in the previous section. Blackadar and Tennekes (1968) summarize the technique, which matches the mean shear in an overlap region where the widely different scales z_o and u_*/f both affect the flow. Since the nondimensional shear is the same by either scaling, a logarithmic velocity profile ensues, which is matched to the empirical surface-layer profile. The result is usually expressed in terms of the nondimensional velocity components parallel and perpendicular to the surface stress, i.e.

$$\mathrm{Re}\,(\dot{\Gamma}) = \mathrm{Re}\left(\frac{\dot{V}}{u_*}\right) = \frac{1}{k}\,(\ln Ro_* - A) \qquad (32)$$

$$\mathrm{Im}\,(\dot{\Gamma}) = -\frac{B}{k} \qquad (33)$$

where $Ro_* = 1/\xi_o = u_*/fz_o$, as before, and A and B are found empirically. The last two drag laws (eq 19 and 27) give the same result as the Blackardar-Tennekes approach: e.g. for eq 27

$$\mathrm{Re}\,(\dot{\Gamma}) = (2k\xi_N)^{-1/2} + \frac{1}{k}(\ln \xi_N - 1) + \frac{1}{k}\ln Ro_*$$

$$\mathrm{Im}\,(\dot{\Gamma}) = -(2k\xi_N)^{-1/2}\,.$$

Hence

$$B = (k/2\xi_N)^{1/2}$$

$$A = -(B + \ln \xi_N - 1)\,.$$

For $\xi_N = 0.045$, the parameters are (for neutral stability) $A = 1.99, B = 2.11$. Conversely, the drag parameters Γ and β may be expressed in terms of A and B by

$$\beta = \tan^{-1}\left\{B/(\ln Ro_* - A)\right\} \qquad (34)$$

$$\Gamma = \frac{1}{k}\,[B^2 + (\ln Ro_* - A)^2]^{1/2}\,. \qquad (35)$$

In naturally occurring boundary layers, buoyancy forces associated with turbulent fluctuations in a nonuniform density field often play an important role in flow dynamics. Generally speaking, in a horizontally homogeneous flow, two new length scales (in addition to z_o and u_*/f) become important when buoyancy effects are considered. They are the depth of the mixed layer and the Obukhov length (see Arya and Sundararajan 1976, for a discussion of the atmospheric analogs). While the former is certainly important when it is small compared to u_*/f, it does not fit easily into the simple theory here. Our previous modeling results (McPhee 1979) suggest that the effect of the pycnocline on mean surface drag is not large under commonly encountered conditions.

The second length scale, L (the Obukhov length), is used to quantify the effect of surface buoyancy flux due to ice growth or ablation. L is obtained (see, for example, Tennekes and Lumley 1972, Chapter 3) by nondimensionalizing the surface-layer turbulent kinetic energy equation such that the nondimensional production rate of turbulent kinetic energy by buoyancy at a particular level z is given by z/L where

$$L = \rho_o u_*^3/(gk\ \overline{\rho' w'}) \tag{36}$$

with $\overline{\rho' w'}$ being the turbulent flux of density fluctuations. When L is positive, turbulence levels are reduced because the eddies must work against gravity; when L is negative turbulence is enhanced. The magnitude of L indicates the scale at which buoyancy is important: e.g., if $|L|$ is very large ($\overline{\rho' w'}$ small) buoyancy has little effect on flow scaling. On the other hand, if $|L|$ is much less than the scale that turbulence would have in the absence of density flux, then the turbulent structure may be completely dominated by buoyancy.

Without examining the complex details of buoyancy-dominated flows, we shall make some generalizations relating to freezing rates based on scaling and show how a simple extension of the theory in the last section has application to conditions of rapid melting.

The equation of state for sea water is approximately

$$\frac{\rho - \rho_o}{\rho_o} = -\alpha(\theta - \theta_0) + \beta(S - S_o)$$

where ρ_o is a reference density at temperature θ_0 and salinity S_0; hence,

$$\frac{\overline{\rho' w'}}{\rho_o} = -\alpha\ \overline{w'\theta'} + \beta\ \overline{w'S'}$$

where $\overline{w'\theta'}$ and $\overline{w'S'}$ are turbulent fluxes of temperature and salinity. When sea water freezes, only a small portion of the dissolved solids (typically about 1/6) are retained in the sea ice matrix, so that a salinity flux occurs as given by

$$\overline{w'S'}\ \Big|_o = -\frac{\rho_{ice}}{\rho_o}\ \frac{(S_w - S_{ice})d}{1000} = -\Delta_s d$$

where d is the ice growth rate and $S_w - S_{ice}$ is the salinity difference in per mille. When ice is growing ($d>0$), heat exchange is entirely latent and $\overline{w'\theta'} = 0$. When ice melts ($d<0$) due to contact with warm water, the interfacial heat flux is $\rho_o c_p \Lambda d$ where Λ is the kinematic latent heat of fusion. Thus

$$\overline{w'\theta'}\ \Big|_o = -\Lambda d \quad [d<0]. \tag{37}$$

The nondimensional Obukhov length, $L_* = fL/u_*$, is

$$L_* = \frac{f}{gk}\ (-\beta\Delta_s + \alpha\Lambda)^{-1}\ \frac{u_*^2}{d}. \tag{38}$$

For temperatures less than 0°C, the thermal expansion coefficient α is negligibly small (but always positive for $S > 24^o/oo$); for water at $\theta = 1°C$, $S = 30^o/oo$, $\alpha \approx 5 \times 10^{-5}\ K^{-1}$ (Neumann and Pierson 1966).

Using typical values ($\beta = 0.8$, $\rho_{ice}/\rho_o = 0.9$, $S_w - S_{ice} = 25^o/oo$, $\Lambda = 65\ K$, $f = 1.4 \times 10^{-4}\ s^{-1}$) in eq 38, for $\theta_w < 0°C$

$$L_* = (-2.0 \times 10^{-5}\ cm^{-1}\ s) \cdot u_*^2/d. \tag{39}$$

For $\theta_w \sim 1°C$, the magnitude of L_* is increased by about 20% by the thermal expansion term.

From the scaling considerations discussed above, we expect L_* to have an impact on the turbulent regime when its magnitude is of the same order or smaller than the neutral nondimensional PBL depth, often taken to be about 0.5. For growth rates such that

$$|d| \geq (4 \times 10^{-5}\ cm^{-1}\ s)\ u_*^2$$

buoyancy, therefore, may affect surface drag. For typical conditions ($u_* \sim 1\ cm\ s^{-1}$) this effect is about 4 cm per day. But freezing rates this high occur only at low temperatures in comparatively thin ice. Under normal circumstances, the drag laws discussed here apply to pack ice that is fairly thick (at least 1 m) and compact (say 80% cover), so an order-of-magnitude estimate suggests that instability associated with surface freezing will rarely have much effect on the average ice drag. Similarly, melting rates encountered in the perennial pack of the central Arctic, where oceanic heat flux is small, cannot be consistently as large as 4 cm day^{-1}, or most of the ice would disappear over a 60-day melt season.

On the other hand, there are conditions under which very rapid melting might have a decided stabilizing effect on the PBL. An example is advection by wind of pack ice across frontal zones at the ice margin where mixed-layer temperature may change by as much as 2 to 3 K within several kilometers.

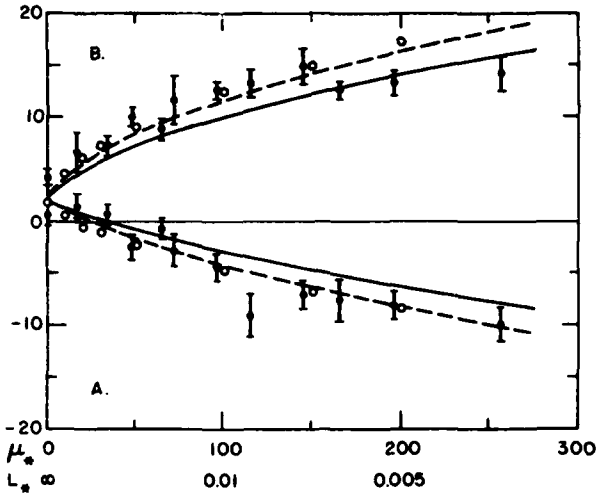

Figure 10. The Rossby-similarity parameters A and B as functions of $\mu_* = 1/L_*$. Data points with error bars are from Clarke and Hess (1974); open circles are from model of Businger and Arya (1974); curves are from present theory with $(R_f)_{max} = 0.2$ (solid) and $(R_f)_{max} = 0.15$ (dashed).

There is some indication at the Bering Sea ice margin that melting rates at least an order of magnitude greater than 4 cm day^{-1} occur when ice moves across such fronts*. If, for example, we were interested in estimating the distance that thick floes might migrate into warm water before melting, then buoyancy would have to be considered in calculating drag. The remainder of this section addresses this problem as an extension of the mixing length approach developed above.

The nondimensional, two-layer theory for a stably stratified flow follows from the idea that the maximum nondimensional mixing length is ξ_N when L_* is infinite (neutral stability), but is proportional to L_* under very stable conditions (L_* small). The simplest expression possessing these limits is

$$\xi_m = \xi_N (1 + \xi_N/\lambda L_*)^{-1} \qquad (40)$$

where λ is a constant yet to be determined. Given L_*, we sutstitute ξ_m for ξ_N in eq 26 and 27 to determine the stress attenuation and to solve for the drag parameters Γ and β, from which the velocity may be obtained.

To evaluate λ, we follow the reasoning of Zilitinkevich (1975). With the surface-layer approximation ($\hat{\tau} = u_* \hat{u}_*$), the flux Richardson number (i.e. the ratio of buoyant production to stress production of turbulent kinetic energy – see Tennekes and Lumley 1972, p. 98) is given by

$$R_f = \left(\frac{g}{\rho_0}\ \overline{\rho' w'}\right) \Big/ \left(u_*^2\ \frac{\partial U}{\partial z}\right) = \frac{1}{k}\left(\frac{fK}{u_*^2}\right)\ \frac{1}{L_*}.$$

The nondimensional eddy viscosity, (fK/u_*^2) in the surface layer is $k\xi$, so we have $\xi = R_f L_*$. Observations show that R_f has an upper limit of about 0.2. For L_* small, eq 40 approaches

$$\xi_m \cong \lambda L_*$$

indicating that $\lambda = (R_f)_{max} = 0.2$.

A comparison of the present theory for two different values of λ with other results is shown in Figure 10, where the Rossby similarity parameters, as defined by eq 32 and 33, are plotted as functions of the variable $\mu_* = 1/L_*$. Also shown are predictions of Businger and Arya (1974), whose model uses a nondimensional eddy viscosity based on the log-linear wind profile determined from the Kansas surface-layer experiment (Businger et al. 1971).

The data points with error bars in Figure 10 are from an analysis by Clarke and Hess (1974) of wind profiles throughout the entire PBL under stable

*Personal communication with C. Pease, NOAA Pacific Marine Environmental Laboratory, 1981.

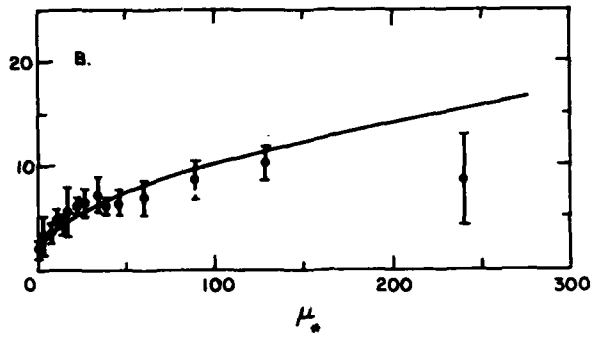

Figure 11. Data from Clarke and Hess (1974) after adjusting u_* *by a constant factor to make neutral values for B agree, compared with present theory with* $(R_f)_{max} = 0.2$.

conditions caused by radiative cooling during the Wangara experiment in the Australian desert.

By applying the same arguments used to deduce the neutral boundary-layer model to a regime in which the maximum mixing length is given by eq 40, it can be shown that the curves in Figure 10 are given exactly by

$$B = (k/2\xi_N)^{1/2}\,(1 + \gamma\mu_*)^{1/2} \tag{41}$$

$$A = 1 - \ln \xi_N - (k/2\xi_N)^{1/2}\,(1 + \gamma\mu_*)^{1/2} + \ln (1 + \gamma\mu_*) \tag{42}$$

where $\mu_* = 1/L_*$ and $\gamma = \xi_N/(R_f)_{max}$.

For $\xi_N = 0.045$ and $(R_f)_{max} = 0.2$, they are

$$B = 2.11\,(1 + 0.22\,\mu_*)^{1/2} \tag{43}$$

$$A = 4.10 - 2.11\,(1 + 0.22\,\mu_*)^{1/2} + \ln (1 + 0.22\,\mu_*)\,. \tag{44}$$

Although at first glance, results for B shown in Figure 10 might indicate that $(R_f)_{max} = 0.2$ is too large, such an interpretation must be approached with caution. Clarke and Hess (1974) point out that their data derive from scaling by u_* as determined at a very smooth site, and one may infer that the u_* to which the entire PBL responds is larger. This point is illustrated in Figure 11, where we have adjusted their data values by applying a constant correction factor to u_* such that their neutral value ($B = 4.3$) agrees with ours ($B = 2.1$). We have assumed that geostrophic wind and surface heat flux measurements are representative, so that ordinate and abscissa values are divided by about 2 and 4, respectively. Apparently, the data are too scattered for one to determine appropriate values for $(R_f)_{max}$, but they do exhibit the same general form as eq 41 and 42.

To recap, given interfacial stress and ice growth rate, we can determine L_* from eq 38 and use the similarity expressions eq 43 and 44 to find β and Γ from eq 34 and 35. For a concrete example, let u_* = 1 cm s^{-1}, d = 50 cm day^{-1}, z_o = 9 cm, and f = 1.23 × 10^{-4} s^{-1} (latitude 58°N); then L_* = 0.037, B = 5.6, A = 0.45, Γ = 21.2, and β = 41°. Compared with the neutral case, the ice travels more than half again as far under similar stress conditions because of the rapid melting.

There is a final ad hoc addition to the theory for which there is at present little experimental justification, but which may be helpful in interpreting data on drift and melt rates near the margins of ice packs. It is useful to consider the physical scales implied in the specific problem above. Regardless of how the PBL depth is defined, similarity of profiles in the outer (Ekman) portion requires that it be proportional to $(k\xi_m)^{1/2}$. (Incidentally, this implies that the PBL depth is proportional to $\mu_*^{-1/2}$ for small L_*, which is again consistent with Businger and Arya (1974) and Zilitinkevich [1975]). In the example above, if the neutral PBL depth is $0.5\,u_*/f$ = 41 m, then the stratified PBL depth is

$$D_s = \left(\frac{\xi_m}{\xi_N}\right)^{1/2} D_N = \left(1 + \frac{\xi_N}{\lambda L_*}\right)^{-1/2} D_N = 15.4 \text{ m}$$

so that the thickness of the boundary layer is much reduced. We may ignore the surface logarithmic layer, since $\xi_m\,u_*/f$ is only about 40 cm (it varies as μ_*^{-1} for large μ_*).

There is no steady-state thermal boundary layer formulation that corresponds with that of the turbulent momentum flux in the outer layer; nevertheless, the maximum mixing length for temperature fluctuations should be of the same order as for momentum, and we have

$$\overline{w'\theta'} \propto -\frac{u_*^2 k \xi_m}{f} \frac{\partial \theta}{\partial z} .$$

If we assume further that the temperature gradient is proportional to $\Delta\theta/D_s$ where $\Delta\theta$ is the difference between the ice melting temperature and the temperature at depth D_s, we obtain an explicit relationship between $\Delta\theta$ and melting rate, i.e.

$$d = -\frac{\overline{w'\theta'}}{\Lambda} = c_1 \frac{k\xi_m (u_*^2/f)\,\Delta\theta}{\Lambda D_s}$$

$$= \frac{2 c_1 k \xi_N}{\Lambda} \left(1 + \frac{\xi_N}{\lambda L_*}\right)^{-1/2} u_* \Delta\theta$$

where we have used

$$D_s = \left(\frac{\xi_m}{\xi_N}\right)^{1/2} (0.5\, u_*/f) .$$

The constant c_1 is unknown, but ought to be of order unity, in which case

$$\Delta\theta = \frac{\Lambda}{2k\xi_N} \left(1 + \frac{\xi_N}{\lambda L_*}\right)^{1/2} \frac{d}{u_*}, \qquad [c_1 = 1] .$$

For the example above, $\Delta\theta = -2.8\ K$, which is not unreasonable for conditions sometimes found near the ice edge. Note that the depth of a pre-existing mixed layer is irrelevant unless it happens to be less than D_s, assuming that the ice advects directly into a mixed layer of uniform temperature above the melting point.

Within the theoretical framework, the constant c_1 could be evaluated experimentally by observing sea surface temperature $\Delta\theta$, surface wind stress (u_*) and ablation rates of large floes drifting across the ice edge front. Whether conditions steady or horizontally homogeneous enough to provide suitable measurements can actually be found is uncertain; but if c_1 were known, knowledge of wind conditions and temperature change across the front—both of which might be sensed remotely—would be enough to make a quantitative estimate of how long floes would survive, how far they would drift, and to what extent they would cool the ocean.

DISCUSSION

An evaluation of several sea-ice drag formulations shows that only those conforming in some way with Rossby-similarity scaling are consistent with the averaged stress magnitude vs relative ice speed relationship determined from the summer AIDJEX data. When such scaling is applied to the classical two-layer approach to the PBL problem, with the added feature that stress is allowed to vary realistically through the inner (surface) layer, an analytic solution is found that reproduces closely the numerical results of McPhee (1979) and of Businger and Arya (1974). The eddy viscosity in the outer (Ekman) layer is given by $K_m = k\xi_N u_*^2/f$ with ξ_N, the maximum dimensionless mixing length, being about 0.045. With this value, the drag law we propose is

$$\dot{\Gamma} = \frac{\dot{V}}{u_*} = 2.5 \ln Ro_* - 4.98) - 5.27\, i \qquad (45)$$

where $Ro_* = fz_o/u_*$. The effective z_o inferred from the AIDJEX results is about 9 cm, but may vary depending on ice characteristics such as ridging intensity or previous melting.

When drifting ice is also melting rapidly, buoyancy affects the drag. This tendency is modeled by a simple extension of the two-layer theory in which the maximum mixing length is reduced from its neutral value as stability increases, eventually becoming proportional to the Obukhov length. With the proportionality constant equal to $(R_f)_{max} = 0.2$, the results are similar to those of Businger and Arya (1974) and are supported by measurements of geostrophic similarity parameters (A and B) in the stable atmospheric PBL reported by Clarke and Hess (1974). Our suggested treatment of the stable PBL, given the growth rate d, is

$$L_* = (-0.17\ \mathrm{cm^{-1}\ s^2})\,(fu_*^2/d)$$

$$B = 2.11\,(1 + 0.22/L_*)^{1/2}$$

$$A = 4.10 - 2.11\,(1 + 0.22/L_*)^{1/2} + \ln(1 + 0.22/L_*)$$

$$\dot{\Gamma} = \frac{\dot{V}}{u_*} = \frac{1}{k}\{(\ln Ro_* - A) - i\,B\} .$$

The results of a specific example, 3, which showed that rapid melting might increase the ice speed by half its neutral value under similar stress conditions, allows us to speculate on the origin of an interesting phenomenon observed near the ice margin in the Bering Sea. According to C. Pease and R. Bourke* it is not uncommon to encounter a continuous band of jumbled, compact floes parallel to the edge of the

*Personal communication with C. Pease, NOAA PMEL, 1981 and R. Bourke, Naval Postgraduate School, 1980.

main pack, but separated from it by several kilometers of open water. Satellite imagery also shows such features occasionally (e.g., see Fig. 3 of Muench and Charnell 1977). Results given in the previous section suggest the following scenario for the formation of such features. Prior to the onset of an off-ice wind event, the ice at the margin of the pack is consolidated and ridged, apparently by wave action and other edge effects. As the wind begins blowing toward open water, the entire pack moves, but the leading floes, drifting into warmer water, accelerate away from the main pack, cooling the water behind them. Thus the leading edge, which was thicker to begin with, experiences less drag at all times, and separates from the main pack more or less intact. As the wind dies, heat flux (which depends on u_*) and melting decrease, so that the band may then persist for some time as a stationary feature.

Whether or not such a situation occurs, the framework presented here, which has a solid basis in PBL theory, at least provides a departure point for interpreting the extremely complex changes in momentum, heat, and salt fluxes that occur across the marginal ice zone.

LITERATURE CITED

Arya, S.P.S., and A. Sundararajan (1976) An assessment of proposed similarity theories for the atmospheric boundary layer. *Boundary-Layer Meteorology*, vol. 10, p. 149-166.

Blackadar, A.K., and H. Tennekes (1968) Asymptotic similarity in neutral planetary boundary layers. *Journal of Atmospheric Science*, vol. 25, p. 1015-1019.

Businger, J.A., and S.P. Arya (1974) The height of the mixed layer in a stably stratified planetary boundary layer. *Advances in Geophysics*, vol. 18A, New York: Academic Press, p. 73-92.

Businger, J.A., J.C. Wyngaard, Y. Izumi, and E.F. Fradley (1971) Flux-profile relationships in the atmospheric surface layer. *Journal of Atmospheric Science*, vol. 28, p. 181-189.

Clark, R.H., and G.D. Hess (1974) Geostrophic departure and the functions A and B of Rossby-number similarity theory. *Boundary-Layer Meteorology*, vol. 7, p. 267-287.

Ekman, V.W. (1905) On the influence of the earth's rotation on ocean currents. *Ark. Mat. Astr. Sys.*, vol. 2, p. 1-52.

Hunkins, K. (1966) Ekman drift currents in the Arctic Ocean. *Deep-Sea Research*, vol. 13, p. 607-620.

Kraus, E. (1977) *Modelling and Prediction of the Upper Layers of the Ocean.* Oxford: Pergamon Press.

McPhee, M.G. (1975) Ice-ocean momentum transfer for the AIDJEX model, AIDJEX Bulletin 29, p. 93-111.

McPhee, M.G. (1979) The effect of the oceanic boundary layer on the mean drift of pack ice: Application of a simple model. *Journal of Physical Oceanography*, vol. 9, p. 388-400.

McPhee, M.G. (1980a) A study of oceanic boundary-layer processes including inertial oscillation at three drifting stations in the Arctic Ocean. *Journal of Physical Oceanography*, vol. 10, p. 870-884.

McPhee, M.G. (1980b) An analysis of pack ice drift in summer. *Sea Ice Processes and Models* (R.S. Pritchard, ed.). Seattle: University of Washington Press, p. 62-75.

McPhee, M.G., and J.D. Smith (1976) Measurement of the turbulent boundary layer under pack ice. *Journal of Physical Oceanography*, vol. 6, p. 696-711.

Muench, R.D., and R.L. Charnell (1977) Observations of medium-scale features along the seasonal ice edge in the Bering Sea. *Journal of Physical Oceanography*, vol. 7, p. 602-606.

Neumann, G., and W.J. Pierson, Jr. (1966) *Principles of Physical Oceanography.* Englewood Cliffs, New Jersey: Prentice-Hall, Inc., p. 545.

Reed, R.J., and W.J. Campbell (1962) The equilibrium drift of Ice Station Alpha. *Journal of Geophysical Research*, vol. 67, p. 281-297.

Rossby, C.G. (1932) A generalization of the theory of the mixing length with application to atmospheric and oceanic turbulence. *Mass. Inst. of Tech. Meteorology Papers*, vol. 1, no. 4.

Rossby, C.G. and R.B. Montgomery (1935) The layer of frictional influence in wind and water current. *Papers, Physical Oceanography and Meteorology, Mass. Institute Technology and Woods Hole Oceanography Institute*, vol. 3, p. 1-100.

Rothrock, D.A. (1975) The steady drift of an incompressible arctic ice cover. *Journal of Geophysical Research*, vol. 80, p. 387-397.

Shuleikin, V.V. (1938) The drift of ice-fields. *Doklady Academy of Sciences, U.S.S.R.*, vol. 19, p. 589-594.

Stern, M.E. (1975) *Ocean circulation physics*, New York: Academic Press, p. 246.

Tennekes, H., and J.L. Lumley (1972) *A first course in turbulence.* Cambridge, Massachusetts: MIT Press.

Zilitinkevich, S.S. (1975) Resistance laws and prediction equations for the depth of the planetary boundary layer. *Journal of Atmospheric Science*, vol. 32, p. 741-752.

A facsimile catalog card in Library of Congress MARC format is reproduced below.

McPhee, Miles G.
Sea ice drag laws and simple boundary layer concepts, including application to rapid melting / by Miles G. McPhee. Hanover, N.H.: U.S. Cold Regions Research and Engineering Laboratory; Springfield, Va.: available from National Technical Information Service, 1982.
iv, 25 p., illus.; 28 cm. (CRREL Report 82-4.)
Prepared for Office of Naval Research by Corps of Engineers, U.S. Army Cold Regions Research and Engineering Laboratory.
Bibliography: p. 17.
1. Boundary air flow. 2. Drag. 3. Drift. 4. Melting. 5. Pack ice. 6. Sea ice. I. United States. Army. Corps of Engineers. II. Army Cold Regions Research and Engineering Laboratory, Hanover, N.H. III. Series: CRREL Report 82-4.


05